

Investigating the origin of Fermi level pinning in Ge Schottky junctions using epitaxially grown ultrathin MgO films

Yi Zhou,^{1,a)} Wei Han,² Yong Wang,³ Faxian Xiu,¹ Jin Zou,³ R. K. Kawakami,² and Kang. L. Wang¹

¹Department of Electrical Engineering, Device Research Laboratory, University of California, Los Angeles, California 90095, USA

²Department of Physics and Astronomy, University of California, Riverside, California 92521, USA

³School of Engineering and Center of Microscopy and Microanalysis, The University of Queensland, Brisbane QLD 4072, Australia

(Received 29 September 2009; accepted 16 February 2010; published online 8 March 2010)

Fermi level (FL) pinning at the Ge valence band results in a high Schottky barrier height for all metal/n-Ge contacts. The origin of this pinning effect has been ascribed to either metal induced gap states or surface states arise from the native defects at the Ge surface, such as dangling bonds. The discrepancy in the reported results/explanations is mainly due to the lack of an explicit characterization of a high quality metal/Ge or metal/ultrathin oxide/Ge junction, which should be ideally single crystalline, atomically smooth and free of process-induced defects or intermixing. We report the Schottky characteristics of high quality metal/MgO/n-Ge junctions with the ultrathin MgO epitaxially grown on Ge. We find the depinning effect displays a weak dependence on the MgO thickness, indicating the interface states due to the native defects on Ge surface are likely to play the dominant role in FL pinning. © 2010 American Institute of Physics.

[doi:10.1063/1.3357423]

Fermi level (FL) pinning inside the Ge band gap leads to a weak dependence of the Schottky barrier height (SBH) on the metal work functions.¹ Even though a few groups have demonstrated depinning of the FL by various methods, an explicit explanation of the underlying mechanism is still unclear. Here “depinning” refers to the shift of the FL with respect to the original strong pinning position. One of the most conjectured origins of pinning is the metal-induced-gap-states (MIGS),^{2,3} which are energy states in the band gap of the semiconductor due to the tailing of the metal electron wave functions into the semiconductor. If MIGS plays the dominant role in FL pinning, inserting an ultrathin oxide (UTO) or insulator between the metal and Ge should depin the FL since the UTO can block the tailing of the metal wave function into Ge and thus reduce the MIGS formation. More importantly, the depinning should be increasingly effective when the UTO thickness is increased until a saturation thickness is reached, at which all MIGS are eliminated. From the MIGS point of view, Nishimura *et al.*⁴ and M. Kobayashi *et al.*⁵ recently demonstrated such an increasing depinning effect with increasing thickness of a thin amorphous insulator (AlO_x, GeO₂, or SiN) between the metal and Ge via sputtering deposition. However, it should be noted that sputtering process could induce defects or intermixing in the films.^{6,7} And the amorphous state of the films could lead to inhomogeneous interfacial structures as well as variations in the bulk film quality and thickness, all of which bring complications to a lucid characterization.⁸ Another possible origin of FL pinning is the surface states which arise from unsatisfied dangling bonds or other defects on the semiconductor surface.^{9,10} Depinning could be achieved by passivating those surface states. Lieten *et al.*¹¹ have shown to depin the FL by inserting a thin Ge₃N₄ layer, either amorphous or

polycrystalline, between the metal and Ge. They attributed the depinning effect to the termination of dangling bonds at the Ge surface by the Ge₃N₄ layer. If surface states play the dominant role in FL pinning, the depinning effect should have a rather weak dependence on the insulator thickness. However, no Ge₃N₄ film thickness dependence of the depinning effect was reported. On the other hand, Ikeda *et al.*¹² have shown to depin the FL by passivating the Ge surface via implantation of sulfur atoms, which act as the dangling bond terminator at the interface. However, implantation induced defects can also bring uncertainties. Therefore, it is evident that a homogenous, epitaxially grown metal/Ge or metal/UTO/Ge junction with a single crystalline order and an atomically smooth morphology is essential to explicitly reveal the FL pinning mechanism.

In this paper, we report the Schottky characteristics of Fe/MgO/n-Ge junctions with the MgO epitaxially grown on Ge. We choose Fe as the Schottky metal due to the fact that it can be epitaxially grown on MgO with an extremely homogenous interface. The entire structure appears to be single crystalline and atomically smooth. The insertion of an ultrathin MgO film can indeed depin the FL, however the SBH displays a negligible dependence on the MgO thickness, suggesting the surface states plays the dominant role in the FL pinning. Further evidence is given by the fact that passivating the surface dangling bonds using aqueous (NH₄)₂S solution depins the FL more effectively than inserting the MgO films.

Samples are grown by molecular beam epitaxy in an ultrahigh vacuum system with a base pressure of 1×10^{-10} torr. The Ge wafers (n type, resistivity of 16–20 Ω cm) are first degreased in isopropyl alcohol, followed by successive washes in dilute NH₄OH₄, H₂SO₄, and H₂O₂. A H₂O₂ wash produces a thin oxide protection layer on the Ge substrate. After loading the substrate into the

^{a)}Electronic mail: yizhou@ee.ucla.edu.

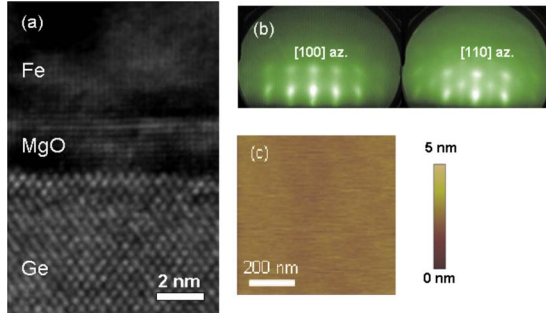


FIG. 1. (Color online) (a) Cross-sectional HRTEM image of a Fe/MgO(3 nm)/n-Ge junction. (b) *in situ* RHEED patterns after the growth of 3 nm MgO. (c) *ex situ* AFM scans after the growth of 3 nm MgO. The root-mean-square roughness is smaller than the atomic spacing of MgO (0.211 nm), indicating the film is atomically smooth.

chamber, it is annealed at 500 °C for 1 h to remove the Ge-oxide layer. The MgO films with various thicknesses (0.5, 1, 2, and 3 nm) are deposited at the substrate temperature of 250 °C by electron beam evaporation of a single crystal MgO source. Then Fe and Al (capping layer) are deposited from thermal effusion cells. The detailed growth method and characterization is published elsewhere.¹³ After growth, Schottky contacts of 300 $\mu\text{m} \times 300 \mu\text{m}$ square size are prepared by conventional photolithography and mesa etching. Ti/Au is deposited on the Ge backside for Ohmic contact.

Figure 1(a) shows the cross-sectional high resolution transmission electron microscopy (HRTEM) image of an Fe/MgO (3 nm)/n-Ge junction. The entire structure displays a single-crystalline order and an atomically smooth morphology, as also evidenced by the sharp *in situ* reflection high energy electron diffraction (RHEED) patterns [Fig. 1(b)] and *ex situ* atomic force microscopy (AFM) scans [Fig. 1(c)] of the MgO after growth. Such a high quality junction with well-defined MgO thicknesses and single crystalline order allows for a reliable characterization of the Schottky characteristics as a function of the MgO thickness.

Figure 2 shows the room temperature J-V characteristics of the Fe/MgO/n-Ge junctions with different MgO thicknesses. With the insertion of the MgO layer, the reverse leakage currents increase as compared to the Fe/n-Ge (without surface passivation, black solid curve), which indicates the

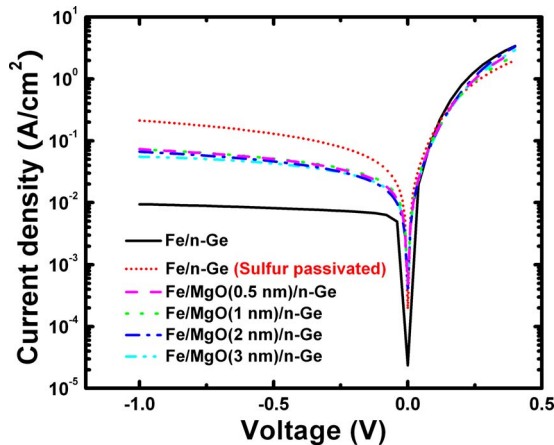


FIG. 2. (Color online) Room temperature J-V characteristics of Fe/MgO/n-Ge diodes with different MgO thicknesses and the Fe/n-Ge diode after sulfur passivation of the Ge surface.

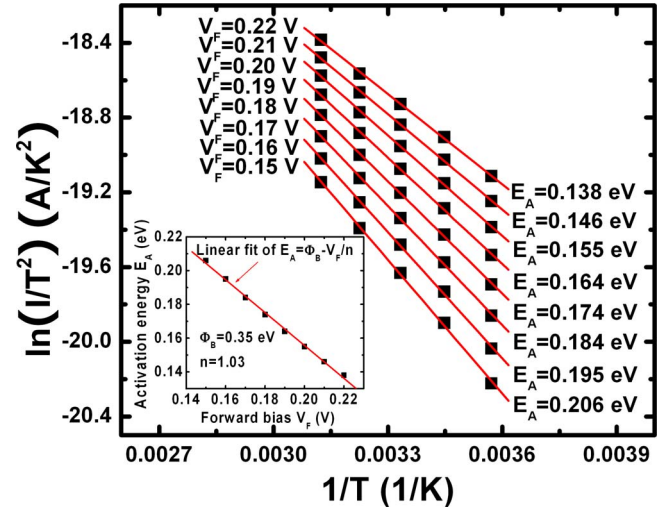


FIG. 3. (Color online) Richardson plots of a Fe/MgO (0.5 nm)/n-Ge diode under different forward biases (0.15–0.22 V). The activation energies (E_A) under each forward bias (V_F) are extracted from the slopes of the linear fits. The inset shows the plot of E_A vs the corresponding V_F , the SBH and ideality factor are extracted from the intercept and slope of the linear fit, respectively.

FL is indeed depinned. However, they display a weak dependence on the MgO thicknesses, which suggests the modulation of SBH by different MgO thickness is negligible.

Temperature dependent forward I-V characterization is performed to extract the SBH and ideality factor n . According to the thermionic emission model, the J-V relation for a Schottky diode under the forward bias ($V_F > 3kT/q$) is given by,¹⁴

$$J = A^* T^2 \exp\left(-\frac{q\Phi_B}{kT}\right) \exp\left(\frac{qV_F}{nkT}\right) \left[1 - \exp\left(-\frac{qV_F}{kT}\right)\right] \approx A^* T^2 \exp\left[-\frac{q}{kT}\left(\Phi_B - \frac{V_F}{n}\right)\right], \quad (1)$$

where A^* is the effective Richardson constant, T is the temperature, q is the electron charge, k is the Boltzmann constant, Φ_B is the effective Schottky barrier height, and V_F is the forward bias voltage. From this equation, the activation energy is given by $E_A = \Phi_B - V_F/n$. When plotting $\ln(J/T^2)$ versus q/kT , also called the Richardson plot, a linear function is found with the slope of E_A . A set of E_A are obtained with different forward bias V_F . Plotting E_A as a function of V_F , a linear curve is obtained with the slope of $-1/n$ and the intercept of Φ_B . For example, Fig. 3 shows the Richardson plots of the Fe/MgO (0.5 nm)/n-Ge under different forward bias (0.15–0.22 V). The activation energy E_A is extracted from the slope of linear fitting of each plot. The E_A is then plotted as a function of V_F as shown in Fig. 3 inset. The Φ_B and n for this particular diode are extracted to be 0.35 eV and 1.03, respectively, from a linear fitting of the plot. It should also be noted that the SBH extracted here is insensitive to the effective Richardson constant A^* . This is especially important to the characterization of junctions with the presence of an ultrathin interfacial insulator, for which the additional contribution from the tunneling probability through the insulator could be viewed as a modification to the conventional A^* .¹⁵

The SBHs of Fe/MgO/n-Ge with MgO thicknesses of 0.5, 1, 2, and 3 nm are extracted to be 0.352, 0.35, 0.363, and

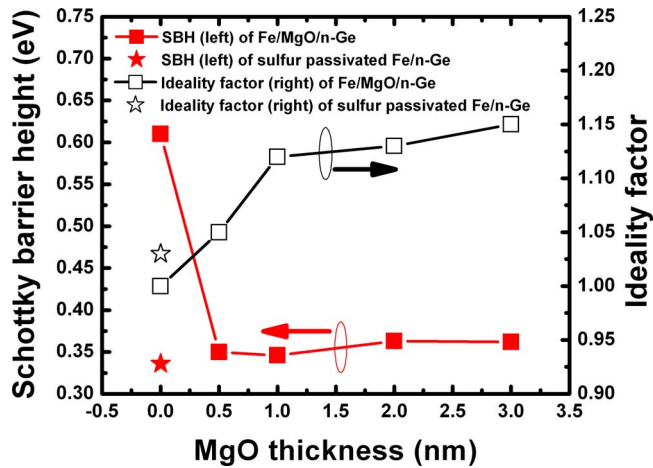


FIG. 4. (Color online) The SBH as a function of the MgO thickness of the Fe/MgO/n-Ge diodes (solid squares to the left axis). The solid star shows the SBH of Fe/n-Ge formed on sulfur passivated Ge. The open squares and star show the ideality factors of the corresponding diode to the right axis.

0.36 eV, respectively, as shown in Fig. 4 in solid red squares to the left axis. The corresponding ideality factors are shown to the right axis in open black squares. Both the SBH and n are values averaged over many diodes on each sample, with a typical root-mean-square-error less than 3%. Such a uniform distribution of the Schottky characteristics benefits from the homogeneous structure of the junctions. Increasing the MgO thickness causes an increase in n , which is consistent with the fact that the transport deviates from pure thermionic emission with the additional tunneling process.¹⁵ However, the dependence of the SBH on the MgO thickness is negligible, which suggests the interface between MgO and Ge plays the dominant role in the Schottky barrier formation. We believe the large density of the surface states at the Ge surface is reduced by the insertion of MgO, which alleviates the FL pinning.

One argument could be that the MgO thicknesses in this study already exceed the saturation thickness and they would have blocked all the MIGS formation. To further confirm the importance of surface states in FL pinning, we investigate the Schottky characteristics of Fe/n-Ge junctions fabricated on a sulfur passivated Ge surface. Before metal deposition, the same n-Ge substrate is dipped into the aqueous $(\text{NH}_4)_2\text{S}$ solution (20%) at 80 °C for 10 min. This treatment is supposed to form a sulfur passivation layer (<3 ML) in which the Ge dangling bonds are saturated by S via bridge-bonding formation.^{16,17} The presence of S at the Ge surface is confirmed by Auger electron spectroscopy as shown in Fig. 5(a). The HRTEM image [Fig. 5(b)] shows an abrupt Fe/Ge interface, without appreciable disorder or intermixing at the interface. Schottky diodes are fabricated and characterized by the same method described above. The depinning effect is found to be more effective than the insertion of MgO, as evidenced by the higher reverse leakage current (dotted red in Fig. 2) and a lower SBH (red star in Fig. 4) for the sulfur passivated Fe/n-Ge diodes. This result further supports that the surface states due to native defects at the Ge surface, rather than the MIGS, plays the dominant role in the FL pinning.

In summary, we investigated the origin of FL pinning in Ge Schottky junctions by characterizing the Fe/MgO/n-Ge

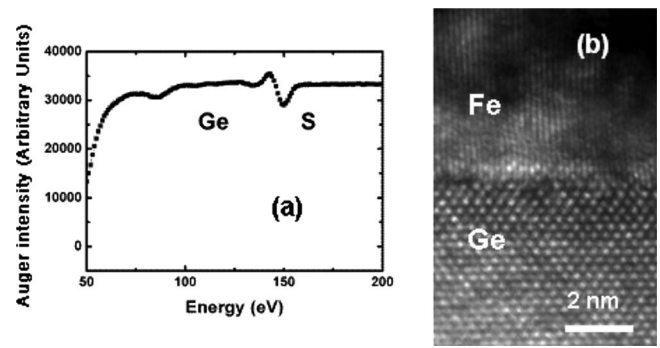


FIG. 5. (a) Auger electron spectrum of the sulfur passivated Ge surface, which confirms the S presence. (b) The HRTEM image of the Fe/n-Ge junction with sulfur passivation.

junctions with single-crystalline and atomically smooth MgO epitaxially grown on Ge. The weak dependence of the SBH on the MgO thickness suggests that the surface states due to native defects at Ge surface are likely to play the dominant role in the FL pinning. Sulfur passivation of the Ge dangling bonds by using aqueous $(\text{NH}_4)_2\text{S}$ solution was shown to be more effective in depinning than insertion of MgO, and this result further supports the dominant role of Ge surface states in FL pinning.

Y.Z. and W.H. contributed equally to this work. Y.Z., F.X., and K.L.W. acknowledge the support from Intel and the Western Institution of Nanoelectronics (WIN) through NRI. W.H. and R.K.K. acknowledge the support of NSF (Grant No. CAREER DMR-0450037). Y.W. and J.Z. acknowledge the support of the Australian Research Council.

¹A. Dimoulas, P. Tsipas, A. Sotiropoulos, and E. K. Evangelou, *Appl. Phys. Lett.* **89**, 252110 (2006).

²V. Heine, *Phys. Rev.* **138**, A1689 (1965).

³S. G. Louie and M. L. Cohen, *Phys. Rev. B* **13**, 2461 (1976).

⁴T. Nishimura, K. Kita, and A. Toriumi, *Appl. Phys. Express.* **1**, 051406 (2008).

⁵M. Kobayashi, A. Kinoshita, K. Saraswat, H.-S. P. Wong, and Y. Nishi, Symposium on VLSI Technology, 2008, p. 54.

⁶W. Njoroge, T. Lange, H. Weis, B. Kohnen, and M. Wuttig, *J. Vac. Sci. Technol. A* **18**, 42 (2000).

⁷E. Simoen, K. Opsomer, C. Claeys, K. Maex, C. Detavernier, R. L. Van Meirhaeghe, and P. Clauws, *J. Electrochem. Soc.* **154**, H857 (2007).

⁸R. T. Tung, *J. Vac. Sci. Technol. B* **11**, 1546 (1993).

⁹W. E. Spicer, I. Lindau, P. R. Skeath, C. Y. Su, and P. W. Chye, *Phys. Rev. Lett.* **44**, 420 (1980).

¹⁰W. E. Spicer, P. W. Chye, P. R. Skeath, C. Y. Su, and I. Lindau, *J. Vac. Sci. Technol.* **16**, 1422 (1979).

¹¹R. R. Lietsen, S. Degroote, M. Kuijk, and G. Borghs, *Appl. Phys. Lett.* **92**, 022106 (2008).

¹²K. Ikeda, Y. Yamashita, N. Sugiyama, N. Taoka, and S. Takagi, *Appl. Phys. Lett.* **88**, 152115 (2006).

¹³W. Han, Y. Zhou, Y. Wang, Y. Li, J. J. I. Wong, K. Pi, A. Swartz, K. M. McCreary, F. Xiu, K. L. Wang, J. Zou, and R. K. Kawakami, *J. Cryst. Growth* **312**, 44 (2009).

¹⁴E. H. Rhoderick and R. H. William, *Metal-Semiconductor Contacts* (Oxford, Clarendon, 1988).

¹⁵S. M. Sze and K. K. Ng, *Physics of Semiconductor Devices*, 3rd ed. (Wiley, New Jersey, 2007).

¹⁶G. W. Anderson, M. C. Hanf, P. R. Norton, Z. H. Lu, and M. J. Graham, *Appl. Phys. Lett.* **66**, 1123 (1995).

¹⁷P. F. Lyman, O. Sakata, D. L. Marasco, T.-L. Lee, K. D. Breneman, D. T. Keane, and M. J. Bedzyk, *Surf. Sci.* **462**, L594 (2000).